Improved Core Loss Calculation for Magnetic Components Employed in Power Electronic Systems

J. Mühlethaler
J. Biela
J. W. Kolar
A. Ecklebe

Improved Core Loss Calculation for Magnetic Components Employed in Power Electronic Systems

J. Mühlethaler[*], J. Biela[†], J. W. Kolar[*], and A. Ecklebe[‡]

[*]Power Electronic Systems Laboratory, ETH Zurich, Email: muehlethaler@lem.ee.ethz.ch
[†]Laboratory for High Power Electronic Systems, ETH Zurich
[‡]ABB Switzerland Ltd., Corporate Research, Baden-Dättwil, Switzerland

Abstract—In modern power electronic systems, voltages across inductors/transformers generally show rectangular shapes, as the voltage across an inductor/transformer can be positive, negative or zero. In the stage of zero applied voltage (constant flux) core losses are not necessarily zero. At the beginning of a period of constant flux, losses still occur in the material. This is due to relaxation processes. A physical explanation about magnetic relaxation is given and a new core loss modeling approach that takes such relaxation effects into consideration is introduced. The new loss model is called i^{2}GSE and has been verified experimentally.

Index Terms—Core Losses, Ferrite, Steinmetz, Relaxation, Dual Active Bridge.

I. INTRODUCTION

In modern power electronic systems, voltages across inductors/transformers generally show rectangular shapes, as illustrated in Fig. 1. The voltage across an inductor / transformer can be positive, negative or zero. This results in the flux in the core ramping up, ramping down or remaining constant.

Core losses need to be determined for the design of inductive components. The most used equation that characterizes core losses is the power equation [1]

$$P_{\mathrm{v}} = k f^\alpha \hat{B}^\beta \qquad (1)$$

where $\hat{B}$ is the peak induction of a sinusoidal excitation with frequency f, P_{v} is the time-average power loss per unit volume, and k, α, β are material parameters. The equation is called the Steinmetz Equation (after Charles P. Steinmetz). The material parameters k, α, and β are accordingly referred to as the Steinmetz parameters. They are valid for a limited frequency and flux density range. The major drawback of the Steinmetz Equation is that it is only valid for sinusoidal excitation. This is a huge drawback, because, as stated above, in power electronic applications the material is usually exposed to non-sinusoidal flux waveforms.

To overcome this limitation, and determine losses for a wider variety of waveforms, different approaches have been developed. The approaches can be classified into the following categories:

1) Improvements of the Steinmetz Equation (1): for instance, the analysis in [2] is motivated by the fact that the loss due to domain wall motion has a direct dependency of $\mathrm{d}B/\mathrm{d}t$. As a result, a modified Steinmetz Equation is proposed. In [3] the approach is further improved and
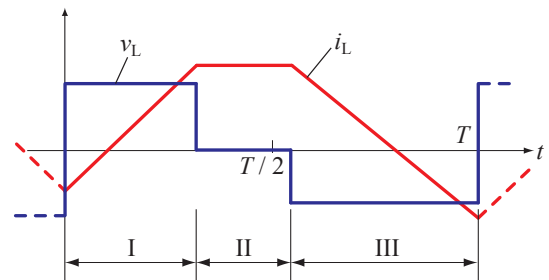

Fig. 1. Typical voltage/current waveform of magnetic components employed in power electronic systems. Phase I: positive voltage; phase II: zero voltage; phase III: negative voltage.

in [4] a method how to deal with minor hysteresis loops is presented and some minor changes on the equation are made. The approach of [2], [3], and [4] leads to the improved Generalized Steinmetz Equation (iGSE)

$$P_{\mathrm{v}} = \frac{1}{T} \int_0^T k_i \left| \frac{\mathrm{d}B}{\mathrm{d}t} \right|^\alpha (\Delta B)^{\beta-\alpha} \, \mathrm{d}t \qquad (2)$$

where ΔB is peak-to-peak flux density and

$$k_i = \frac{k}{(2\pi)^{\alpha-1} \int_0^{2\pi} |\cos\theta|^\alpha 2^{\beta-\alpha} \mathrm{d}\theta}. \qquad (3)$$

The parameters k, α, and β are the same parameters as used in the Steinmetz Equation (1). By use of the iGSE losses of any flux waveform can be calculated, without requiring extra characterization of material parameters beyond those for the Steinmetz Equation.

2) Calculation of the losses with a loss map that is based on measurements. This loss map stores the loss information for different operating points, each described by the flux density ripple ΔB, the frequency f, the temperature T, and a DC bias H_{DC} (e.g. in [5]–[7]).

3) Methods to determine core losses based on breaking up the total loss into loss components, i.e. hysteresis losses, classical eddy current losses, and residual losses [8].

4) Hysteresis models such as Preisach and Jiles-Atherton used for calculating core losses.

In the categories 1 and 2 a loss energy is assigned to each section of the voltage / current waveform as illustrated in Fig. 1 (e.g. via an equation as (2) or via a loss map), and these

losses are summed-up to calculate the power loss occurring in the core. This approach is e.g. implemented in [9].

In most of the previous publications, the phase where the voltage across the magnetic component is zero has not been discussed. It has been implicitly assumed that no losses occur when the flux remains constant. However, as measurements show, this is not a valid simplification. At the beginning of a period of constant flux, losses still occur in the material. In the publication [10] about core loss modeling, a loss increase during zero voltage periods has been observed, however, no explanation or modeling approach is given.

This work shows that this loss increase is due to relaxation processes inside the magnetic core material. Furthermore, a new model is introduced that considers relaxation effects when calculating core losses. A core loss measurement test setup has been built to analyze core losses under general flux waveform excitations. The test system is presented in **Section II**. In **Section III** a brief introduction to magnetic relaxation is given. In **Section IV**, **V**, and **VI** a new loss model is derived that substantially improves core loss calculation by taking relaxation processes into consideration. In **Section VII** an easy-to-follow example is given to illustrate how the new model can be applied. Before concluding the work, in **Section VIII** a short discussion of the behavior of different materials is given.

II. TEST SETUP TO MEASURE CORE LOSSES

In order to perform core loss measurements, the best measurement technique has to be selected first. In [11] different methods are compared. The B-H Loop Measurement has been evaluated as the most suitable. Amongst other advantages, this technique offers rapid measurement (compared to other methods, e.g. calorimetric measurements), copper losses are not measured, and a good accuracy. The principle is as follows: two windings are placed around the Core Under Test (CUT). The sense winding (secondary winding) voltage v is integrated to sense the core flux density B

$$B(t) = \frac{1}{N_2 \cdot A_{\mathrm{e}}} \int_0^t v(\tau) \mathrm{d}\tau \qquad (4)$$

where N_2 is the number of sense winding turns and A_{e} is the effective core cross section of the CUT. The current in the excitation winding (primary winding) is proportional to the magnetic field strengths H

$$H(t) = \frac{N_1 \cdot i(t)}{l_{\mathrm{e}}} \qquad (5)$$

where N_1 is the number of excitation winding turns and l_{e} is the effective magnetic path length of the CUT. The loss per unit volume is then the enclosed area of the B-H loop, multiplied by the frequency f

$$\frac{P}{V} = f \oint H \mathrm{d}B. \qquad (6)$$

The selected approach is widely used [4], [6]. The built test system consists of a power stage, a power supply, an oscilloscope and a heating chamber. It is controlled by a
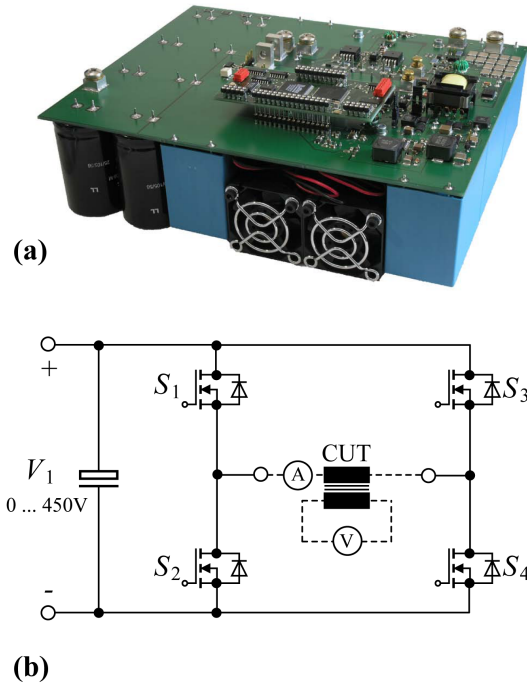

(a)

(b)

Fig. 2.   Test setup (a) photograph, (b) simplified schematic.

MATLAB program running on the oscilloscope under Microsoft Windows. In Fig. 2 a photograph (a) and the simplified schematic (b) of the power stage are shown. The power stage is capable of a maximal input voltage of $450\,\mathrm{V}$, output current of $25\,\mathrm{A}$ and a switching frequency of up to $200\,\mathrm{kHz}$. The test setup allows application of a general rectangular voltage shape across the CUT that leads to a triangular and / or trapezoidal current shape including a DC bias (if desired).

The reader is referred to [12] for more information about the test setup, including a detailed accuracy analysis of the loss measurement.

III. RELAXATION PROCESSES IN MAGNETIC MATERIALS

As already mentioned in the introduction, during the phase of constant flux (where the voltage across the magnetic component is zero) losses still occur in the core material. A literature survey led to the conclusion that this is due to relaxation processes in the magnetic core material. In this section, first measurements are presented that illustrate magnetic relaxation. Further, an attempt to theoretically explain the effect is given, and, with it, the resulting shape of a B-H loop for trapezoidal flux waveform is analyzed.

A. Measurement Results

According to (2), the energy loss would only depend on the magnitude and the slope of the flux, and, consequently, there should be no loss during periods of constant flux (zero voltage). Measurements on waveforms as illustrated in Fig. 3(a) have been performed to investigate this. Fig. 4 shows
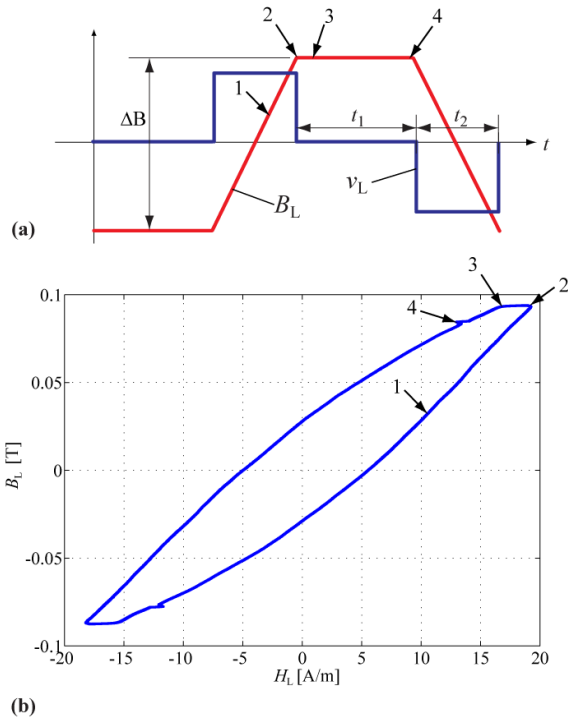
(a)

(b)

Fig. 3. (a) Voltage and flux density waveforms. (b) B-H loop to illustrate magnetic relaxation under trapezoidal flux shape condition.
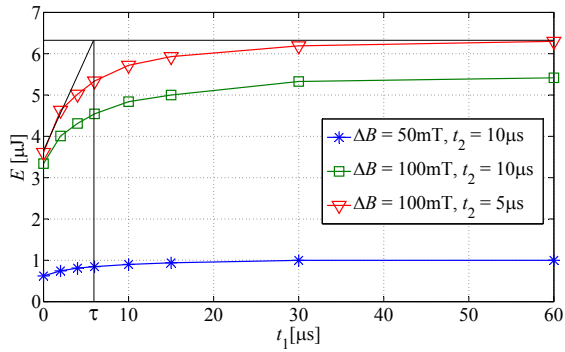

Fig. 4. Measurement results measured on ferrite EPCOS N87 (R42, B64290L22X87 [13]). It is further illustrated how τ according to (18) can be extracted.

the corresponding measurement results. The CUT is made of ferrite EPCOS N87 (size R42). According to (2), the duration of t_1 should not influence the loss *energy* per cycle, but, as can be seen, increasing t_1 has a substantial influence on the loss energy per cycle. In particular, a change in t_1 at low values of t_1 influences the dissipated loss. For larger values of t_1, the core material has time to reach its equilibrium state and no increase in losses can be observed when t_1 is further increased.

It has been confirmed that this effect is *not* due to an impact of the measurement setup (e.g. small exponential change of current due to voltage drop over the inductor in the zero voltage time intervals).

Concluding, at the beginning of the phase of constant flux (where the voltage across the magnetic component is zero) losses still occur because of relaxation processes in the magnetic core material. Next, a brief introduction about magnetic relaxation is given.

B. Theory of Relaxation Effects

There are basically three physical loss sources: (static) hysteresis losses, eddy-current losses, and a third loss component which is often referred to as residual losses. Hysteresis losses are linear with the frequency f (rate-independent B-H loop). Eddy-current losses occur because of an induced current due to the changing magnetic field, and are strongly depend on the material conductivity and the core geometry. The residual losses are, according to [8], due to relaxation processes: if the thermal equilibrium of a magnetic system changes, the system progressively moves towards the new thermal equilibrium condition. When the magnetization changes rapidly, as for example is the case in high-frequency or pulsed field applications, such relaxation processes become very important.

The *Landau-Lifshitz* Equation qualitatively describes the dynamics of the magnetic relaxation process. The equation follows directly from equating the rate of change of the angular momentum L to the torque $\mathrm{M} \times \mathrm{H}$ reduced by a frictional term that is directed opposite to the direction of motion [8]:

$$\frac{\mathrm{d}\mathbf{M}}{\mathrm{d}t} = \gamma \mathbf{M} \times \mathbf{H} - \Lambda \mathbf{M} \times (\mathbf{M} \times \mathbf{H})/M^2, \qquad (7)$$

where $\gamma = ge/2mc$ is the magnetomechanical ratio M/L, $\mathbf{M}$ is the magnetization vector, $\mathbf{H}$ the magnetic field vector, and Λ is called the relaxation frequency. It describes how the system progressively moves towards the new thermal equilibrium. The equilibrium is achieved by rearranging the magnetic domain structures to reach states of lower energy. The relaxation process limits the speed of flux change, hence the B-H loops becomes rate-dependent. Several physical processes are contributing simultaneously to magnetic relaxation. The interested reader is referred to [8], [14], [15] for more information.

Concluding, due to *magnetic relaxation*, the magnetization may change even when the applied field is constant (the magnetization is delayed). Consequently, a residual energy loss still occurs in the period of a constant applied field. Furthermore, the shape of the hysteresis loop is changed depending on the rate of change of the applied field (rate-dependent loop). An analysis of the impact of *magnetic relaxation* to a trapezoidal flux shape now follows.

C. Shape of B-H Loop for Trapezoidal Flux Waveforms

A B-H loop under trapezoidal flux waveform condition has been measured to gain a better comprehension of why the losses increase when the duration of the zero voltage period is increased. The CUT is a toroid core R42 made of ferrite EPCOS N87. In Fig. 3(a) the flux waveform, and in Fig. 3(b) the corresponding B-H loop are plotted. The B-H loop always traverses counterclockwise. The different instants (cf. numbers in Figure 3(a) and (b)) are now discussed step-by-step:

1) A constant voltage at the CUT primary winding results in a time linear flux increase.
2) The CUT primary voltage is set to zero; as a consequence the flux is frozen ($dB/dt = 0$). However, the material has not yet reached its thermal equilibrium. The magnetic field strength H declines to move towards the new thermal equilibrium and therewith reaches a state of lower energy. This can also be observed in the current (the current declines accordingly).
3) This point is reached approximately $24\,\mu s$ after point 2. It is the point of the new thermal equilibrium.
4) This point is reached approximately $200\,\mu s$ after point 3. The demagnetization in the zero voltage period is due to the small voltage drop over the on-resistance of the MOSFETs and copper resistance of the inductor primary winding. This demagnetization follows a completely different time constant than the demagnetization due to relaxation losses (cf. the approximately same distance 2-3 and 3-4, but the completely different time scale). At point 4 a negative voltage is applied to the CUT. The small buckle in the B-H loop is due to small capacitive currents at the switching instant.

The period between point 2 and 3 obviously increases the area of the B-H loop, and therewith increases the core losses. The loop area increases as a function of the duration t_1. After the thermal equilibrium is reached (in the above example after approximately $24\,\mu s$) the loss increase becomes (almost) zero. More measurements are presented to find a method to include this effect into an existing core loss model in the next section.

IV. Model Derivation 1: Trapezoidal Flux Waveform

Losses can be calculated with (2), without requiring extra characterization of material parameters beyond the parameters for the Steinmetz Equation. The Steinmetz parameters are often given by core manufacturers, hence core loss modeling is possible without performing extensive measurements. However, the approach has some drawbacks. First, it neglects the fact that core losses may vary under DC bias condition. This is discussed in [12], where a graph showing the dependency of the Steinmetz parameters (α, β and k) on premagnetization is introduced. With it, losses can be calculated via the Steinmetz Equation (1) or the iGSE (2) using appropriate Steinmetz parameters. Another source of inaccuracy is that relaxation effects are not taken into consideration. As approach (2) is very often discussed in literature and often applied for designing magnetic components, improving this method would have the most practical use. Furthermore, in [16] it has been evaluated as the most accurate state-of-the-art loss model based on Steinmetz parameters. For this two reasons, in the following, the iGSE will be extended to consider relaxation losses as well.

Plotting the losses with logarithmic axes, where the x-axis represents the frequency, and the y-axis represents the power loss, leads to an approximately straight line. This is because the losses follow a power function, as e.g. the law stated in (1)
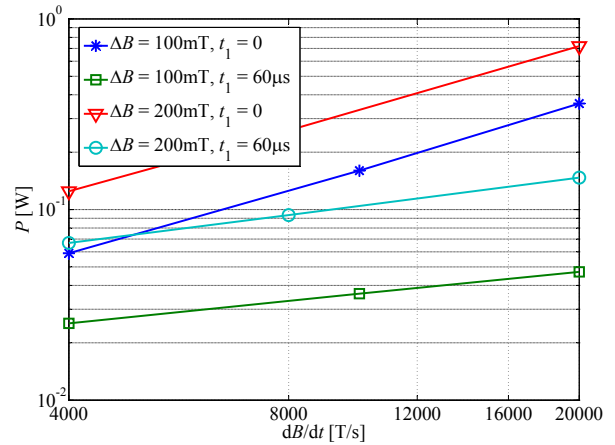
Fig. 5. Core Loss (ferrite N87; measured on R42 core), $T = 25\,^\circ\mathrm{C}$.

is. The parameter α of (1) represents the slope of the curve in the plot. In Fig. 5 such plots are given for few operating points. Instead of the frequency f, dB/dt has been used as x-axis, which, for symmetric triangular or trapezoidal flux waveforms, is directly proportional to the frequency f. The time t_1 is defined as in Fig. 3 ($t_1 = 0$ leads to a triangular flux waveform). It is very interesting to note that when a long zero voltage phase is added between two voltage pulses (having a flux waveform as given in Fig. 3) the loss still follows a power function. The same conclusion can be made when keeping dB/dt constant and varying ΔB, hence, the use of a power function with variable ΔB is justified as well.

It should be pointed out that when having a zero voltage interval ($t_1 \neq 0$) the average power loss decreases (cf. Fig. 5). There is no discrepancy with the observation in Fig. 4, where an *energy loss per cycle* increase has been observed. When having a zero voltage interval the energy loss per cycle increases, but the period increases as well and leads to a lower average power loss.

The approach of (2) will now be extended by taking relaxation effects into consideration. This is done by adding a new additional term that represent the relaxation effect of a transition to zero voltage. As can be seen in Fig. 4, the loss energy can be modeled with the exponential equation

$$E = \Delta E \left(1 - e^{-\frac{t_1}{\tau}}\right), \qquad (8)$$

where ΔE is the maximum loss energy increase (which occurs, when the magnetic material has enough time to reach the new thermal equilibrium), τ is the relaxation time that has to be further determined, and t_1 is the duration of the constant flux (zero applied voltage) phase. The exponential behavior is typical for relaxation processes. Measurements have shown that τ can be considered as a constant parameter for different operating points. ΔE is a function of ΔB and $dB(t)/dt$, where ΔB and $dB(t)/dt$ define the flux density waveform before a transition to zero voltage as illustrated in Fig. 6. As mentioned before, and illustrated in Fig. 5, the losses
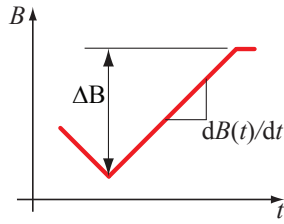
Fig. 6.   Definition of $\mathrm{d}B(t)/\mathrm{d}t$ and ΔB.

Fig. 7.   Triangular flux density waveform.

Fig. 8.   Core loss duty cycle dependency. $\Delta B = 0.1\,\mathrm{T}$, $f = 20\,\mathrm{kHz}$.

with and without zero voltage phase follow a power function. Consequently, the losses due to relaxation must follow a power function as well. Because τ is constant and the energy in all operating points follow the same law stated in (8), the energy ΔE has to follow a power function as well[1] (with variables ΔB and $\mathrm{d}B(t)/\mathrm{d}t$). As a consequence, the following power function can be defined for ΔE:

$$\Delta E = k_{\mathrm{r}} \left| \frac{\mathrm{d}}{\mathrm{d}t} B(t) \right|^{\alpha_{\mathrm{r}}} (\Delta B)^{\beta_{\mathrm{r}}}, \qquad (9)$$

where α_{r}, β_{r}, and k_{r} are new model parameters that have to be determined empirically. The relaxation losses of a transition to zero voltage can be determined according to the antecedent flux density slope $\mathrm{d}B(t)/\mathrm{d}t$ and the antecedent flux density peak-to-peak value ΔB. Accordingly, when the flux density reaches and remains at zero as occurs e.g. in a buck converter that is operating in discontinuous conduction mode, relaxation losses have to be taken into consideration as well. However, the losses *may* (slightly) differ in this situation because the antecedent flux density is DC biased. This DC level of the antecedent flux density has not been part of investigation of the present work and could be investigated as part of a future work.

Concluding, (2) has been extended by an additional term that describes the loss behavior for a transient to constant flux. This leads to a new model

$$P_{\mathrm{v}} = \frac{1}{T} \int_0^T k_i \left| \frac{\mathrm{d}B}{\mathrm{d}t} \right|^{\alpha} (\Delta B)^{\beta - \alpha} \, \mathrm{d}t + \sum_{l=1}^{n} P_{\mathrm{r}l}, \qquad (10)$$

where $P_{\mathrm{r}l}$ represents the power loss density due to the lth of n transients to zero voltage. Each transient to zero voltage is calculated according to

$$P_{\mathrm{r}l} = \frac{1}{T} k_{\mathrm{r}} \left| \frac{\mathrm{d}}{\mathrm{d}t} B(t) \right|^{\alpha_{\mathrm{r}}} (\Delta B)^{\beta_{\mathrm{r}}} \left(1 - \mathrm{e}^{-\frac{t_1}{\tau}} \right). \qquad (11)$$

V. MODEL DERIVATION 2: TRIANGULAR FLUX WAVEFORM

Often in power electronics, one has a period of zero voltage applied to a magnetic component winding, e.g. in the transformer of a bidirectional isolated DC-DC converter with Dual Active full Bridges (DAB). A DAB will be presented in Section VII as an example to illustrate the model. In this case, (10) can directly be used to improve the loss model.

---

[1]Power loss and energy loss are coupled by a time factor. Because τ is constant, this factor is the same for all operating points and the function structure remains.
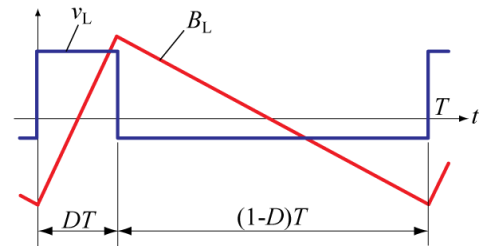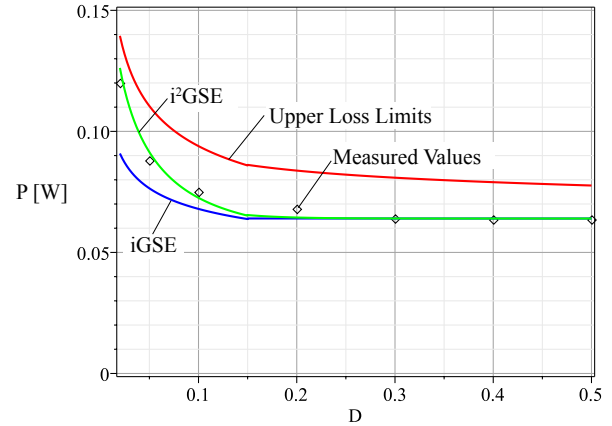
However, another frequently occurring waveform is a triangular flux waveform in which the flux slope changes to another *nonzero* value. This case is illustrated in Fig. 7. When assuming a duty cycle of $50\,\%$ ($D = 0.5$), directly after switching to the opposite voltage the flux slope reverses, the material has hardly time to move towards the new thermal equilibrium. As a consequence, no notable loss increase is expected and thus this case is well described by the iGSE (2). However, when the duty cycle goes to smaller values, once each period, a high flux slope is followed by a very slow flux change. Assuming D to be infinitely small, a switch to a constant flux happens. Consequently, in this case the iGSE (2) is not accurate and the relaxation term has to be added. In all operating points where $D > 0$ and $D < 0.5$ (or $D > 0.5$ and $D < 1$), a behavior that is in-between these two cases is expected. In other words, only part of the relaxation term has to be added.

In Fig. 8 the calculated and measured core losses as a function of the duty cycle are plotted. One calculation has been performed based on the iGSE (2) which, according to the above discussion, represents the lower limit of possible losses (as no relaxation effects are taken into account). It should be noted that two sets of Steinmetz parameters have been used for the calculation of the iGSE. The reason is that the Steinmetz parameters are only valid in a limited $\mathrm{d}B/\mathrm{d}t$ range, and the $\mathrm{d}B/\mathrm{d}t$ in this experiment is varying in a wide range. This explains the sharp bend of the iGSE curve at $D = 0.15$ (change of Steinmetz parameter). Another calculation has been

made always including the full relaxation loss term and which represents the upper loss loss limit. In other words, it can be said that losses are expected to have values between the line representing the upper loss limit and the line representing the lower loss limit (iGSE). According to the previous discussion, the real losses are closer to the lower loss limit for D close to 0.5, and losses closer to the upper loss limit for D close to zero. This has been confirmed by measurements as can be seen in Fig. 8. Other operating points showed the same behavior.

Based on the above discussion, the new approach can be further improved to be also valid for triangular flux waveforms. Basically, (10) can be rewritten as

$$P_{\mathrm{v}} = \frac{1}{T} \int_0^T k_i \left| \frac{\mathrm{d}B}{\mathrm{d}t} \right|^\alpha (\Delta B)^{\beta-\alpha} \, \mathrm{d}t + \sum_{l=1}^n Q_{\mathrm{r}l} P_{\mathrm{r}l}, \quad (12)$$

where $Q_{\mathrm{r}l}$ has to be further defined. In the case of a switch to zero voltage, $Q_{\mathrm{r}l}$ needs to have the value 1. Furthermore, it has to have a structure so that (12) fits the measurement points of a duty cycle measurement, such as illustrated in Fig. 8. The following function has been chosen:

$$Q_{\mathrm{r}l} = \mathrm{e}^{-q_{\mathrm{r}} \left| \frac{\mathrm{d}B(t_+)/\mathrm{d}t}{\mathrm{d}B(t_-)/\mathrm{d}t} \right|}, \quad (13)$$

where $\mathrm{d}B(t_-)/\mathrm{d}t$ represents the flux density before the switching, $\mathrm{d}B(t_+)/\mathrm{d}t$ the flux density after the switching, and q_{r} is a new material parameter. For a triangular waveform, as illustrated in Fig. 7, (13) can be rewritten (for $D \leq 0.5$)

$$Q_{\mathrm{r}l} = \mathrm{e}^{-q_{\mathrm{r}} \frac{\frac{\Delta B}{(1-D)T}}{\frac{\Delta B}{DT}}} = \mathrm{e}^{-q_{\mathrm{r}} \frac{D}{1-D}}. \quad (14)$$

In the case of the material Epcos N87 $q_{\mathrm{r}} = 16$ has been found, the resulting loss curve is plotted in Fig. 8. Before giving an illustrative example in Section VII, the new model will be summarized and the steps to extract the model parameters will be given.

VI. New Core Loss Model: The i²GSE

A new loss model that substantially increases the expected accuracy when core losses are modeled has been introduced. We call this new model the *improved-improved Generalized Steinmetz Equation* i²GSE. The name has been chosen because it is an improved version of the iGSE [4]. The power loss density can be calculated with

$$P_{\mathrm{v}} = \frac{1}{T} \int_0^T k_i \left| \frac{\mathrm{d}B}{\mathrm{d}t} \right|^\alpha (\Delta B)^{\beta-\alpha} \, \mathrm{d}t + \sum_{l=1}^n Q_{\mathrm{r}l} P_{\mathrm{r}l}, \quad (15)$$

where $P_{\mathrm{r}l}$ is calculated for each voltage change according to

$$P_{\mathrm{r}l} = \frac{1}{T} k_{\mathrm{r}} \left| \frac{\mathrm{d}}{\mathrm{d}t} B(t) \right|^{\alpha_{\mathrm{r}}} (\Delta B)^{\beta_{\mathrm{r}}} \left(1 - \mathrm{e}^{-\frac{t_1}{\tau}} \right), \quad (16)$$

$Q_{\mathrm{r}l}$ is a function that further describes the voltage change and is

$$Q_{\mathrm{r}l} = \mathrm{e}^{-q_{\mathrm{r}} \left| \frac{\mathrm{d}B(t_+)/\mathrm{d}t}{\mathrm{d}B(t_-)/\mathrm{d}t} \right|}, \quad (17)$$

and α, β, k_i, α_{r}, β_{r}, k_{r}, τ, and q_{r} are material parameters.

Now, the steps to extract the model parameters are given:

1) First, the parameters k_i, α, and β are extracted. The core is excited with a rectangular voltage waveform that leads to a symmetric triangular flux waveform. Measurements at three operating points are performed, then (15) is solved for the three parameters. For triangular flux waveform we have $\sum_{l=1}^n Q_{\mathrm{r}l} P_{\mathrm{r}l} = 0$ (no phase of zero applied voltage). In Table I the measurement results and the corresponding parameters are given. These parameters could be extracted directly from the data sheet as well, as explained in [4].

2) The parameter τ can be read from Fig. 4 with

$$\frac{\Delta E}{\tau} = \frac{\mathrm{d}E}{\mathrm{d}t}, \quad (18)$$

where $\mathrm{d}E/\mathrm{d}t$ represents the slope of the energy increase directly after switching to zero voltage. This is illustrated in Fig. 4. $\tau = 6 \, \mu\mathrm{s}$ has been extracted for the material N87.

3) The parameters k_{r}, α_{r}, and β_{r} are extracted by performing measurements at three operating points with t_1 large enough to let the material reach the thermal equilibrium. Then, (9) is solved for the three parameters. In Table I the measurement results and the corresponding parameters are given.

4) The parameter q_{r} has to be selected such that (15) fits the measurement points of a duty cycle measurement, as illustrated in Fig. 8.

All model parameters are summarized in Table I. Extracting the parameters is sometimes difficult and measurements have to be performed very carefully. One error source is a possible current decrease due to a voltage drop over the inductor winding during "zero" voltage phase. This can be avoided by choosing a high amount of primary turns. This increases the inductance value and the current is kept more constant (by choosing a high amount of primary turns the winding copper resistance increases as well, however, the inductance value increases quadratically while the resistance value increases linearly).

TABLE I
MEASUREMENT RESULTS AND MODEL PARAMETER OF MATERIAL EPCOS N87.

Operating Point (ΔB; f)	Loss Density [kW/m³]	Model Parameters
(0.1 T; 20 kHz)	5.98	$k_i = 8.41$
(0.1 T; 50 kHz)	16.2	$\alpha = 1.09$
(0.2 T; 50 kHz)	7.28	$\beta = 2.16$
(ΔB; $\mathrm{d}B(t)/\mathrm{d}t$)	[J/m³]	
(0.1 T; 4 kT/s)	0.068	$k_{\mathrm{r}} = 0.0574$
(0.1 T; 20 kT/s)	0.13	$\alpha_{\mathrm{r}} = 0.39$
(0.2 T; 20 kT/s)	0.32	$\beta_{\mathrm{r}} = 1.31$
		$\tau = 6 \, \mu\mathrm{s}$
		$q_{\mathrm{r}} = 16$

VII. Example of How to Use the New Model

In the previous section, a new core loss modeling approach was introduced. This section shows now an easy-to-follow
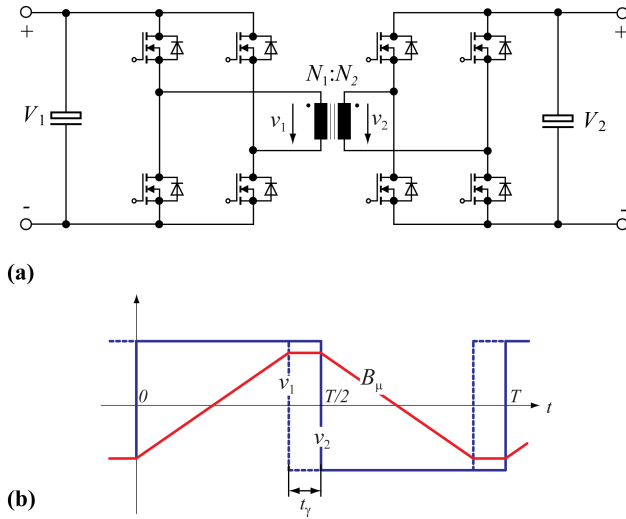
(a)

(b)

Fig. 9. DAB schematic (a) and waveforms (b) with specifications given in Table II.

TABLE II
SPECIFICATIONS OF DAB TRANSFORMER

$V_{\mathrm{DC}} = V_1 = V_2$	42 V
f	50 kHz
N=N_1=N_2	20
Effective Magnetic Length l_{e}	103 mm
Effective Magnetic Cross Section A_{e}	95.75 mm^2
Core	EPCOS N87, R42 (B64290L22X87) [13]

example that illustrates how to calculate core losses of a transformer employed in a bidirectional isolated DC-DC converter with Dual Active full Bridges (DAB) [16], [17]. In Fig. 9(a) the simplified schematic and in Table II the specifications of the transformer are given. The shape of the core influences the core losses, however, this is not the scope of the present work, hence a simple toroid is considered as the transformer core. Phase-shift modulation has been chosen as modulation method: primary and secondary full bridge switch with 50 % duty cycle to achieve a rectangular voltage v_1 and v_2 across the primary and secondary transformer side, respectively. The waveforms are illustrated in Fig. 9(b), including the magnetic flux density B_μ of the transformer core. A phase shift γ between v_1 and v_2 results in a power transfer. When the voltages v_1 and v_2 are opposed (which is the case in phase t_γ), the full voltage drop is across the transformer leakage inductance and the magnetic flux density B_μ remains unchanged.

Only the magnetic flux density B_μ time behavior has been considered for designing the transformer, i.e. no winding losses or leakage inductance have been calculated. The value of the leakage inductance is very important for the functionality, however, it is not discussed here. Therefore, no statement about feasibility is made, the circuit should only represents solely a simple and easy-to-follow illustrative magnetic example.

The losses are calculated according to the i^{2}GSE (15). The results are then compared with measurement results. The peak flux density in the core can be calculated with [16]

$$\hat{B} = \frac{1}{2}\frac{V_{\mathrm{DC}}}{NA_{\mathrm{e}}}\left(\frac{T}{2} - t_\gamma\right) \tag{19}$$

and its time derivative with

$$\frac{\mathrm{d}B}{\mathrm{d}t} = \begin{cases} \frac{V_{\mathrm{DC}}}{NA_{\mathrm{e}}} & \text{for } t \geq 0 \text{ and } t < \frac{T}{2} - t_\gamma, \\ 0 & \text{for } t \geq \frac{T}{2} - t_\gamma \text{ and } t < \frac{T}{2}, \\ -\frac{V_{\mathrm{DC}}}{NA_{\mathrm{e}}} & \text{for } t \geq \frac{T}{2} \text{ and } t < T - t_\gamma, \\ 0 & \text{for } t \geq T - t_\gamma \text{ and } t < T. \end{cases} \tag{20}$$

Calculating the losses according to (15) leads to the following expression as a function of t_γ

$$P = \frac{T - 2t_\gamma}{T}k_i \left| \frac{V_{\mathrm{DC}}}{NA_{\mathrm{e}}} \right|^\alpha \left| \frac{V_{\mathrm{DC}}}{NA_{\mathrm{e}}}\left(\frac{T}{2} - t_\gamma\right) \right|^{\beta - \alpha} A_{\mathrm{e}}l_{\mathrm{e}}$$
$$+ A_{\mathrm{e}}l_{\mathrm{e}}\sum_{l=1}^{n} Q_{\mathrm{r}l}P_{\mathrm{r}l}, \tag{21}$$

where $\sum_{l=1}^{2} Q_{\mathrm{r}l}P_{\mathrm{r}l}$ represents the two transients to zero voltage. There are two switching instants to zero voltage, each with $Q_{\mathrm{r}l} = 1$. The values for $P_{\mathrm{r}l}$ then have to be determined: it is for each transient

$$P_{\mathrm{r}l} = \frac{1}{T}k_{\mathrm{r}} \left| \frac{V_{\mathrm{DC}}}{NA_{\mathrm{e}}} \right|^{\alpha_{\mathrm{r}}} \left| \frac{V_{\mathrm{DC}}}{NA_{\mathrm{e}}}\left(\frac{T}{2} - t_\gamma\right) \right|^{\beta_{\mathrm{r}}} \left(1 - \mathrm{e}^{-\frac{t_\gamma}{\tau}}\right). \tag{22}$$

The losses have been calculated according to the new approach, and have been compared to a calculation using the classic iGSE (2) and with measurement results. Open-circuit (no load) measurements have been performed to validate the new model: the primary winding is excited to achieve a flux density as illustrated in Fig. 9(b). Measurements for different values of t_γ have been performed, at constant frequency f and voltage V_{DC}. The new model and measurement results match very well as shown in Fig. 10.

In [16] different state-of-the-art core loss calculation approaches are compared using a very similar example. The iGSE (2) showed the best agreement with measurements, but for increasing zero voltage periods t_γ, the calculated core losses start deviating from the measured core losses. The reason becomes clear with the new approach i^{2}GSE and the calculation can be improved.

VIII. MEASUREMENTS ON DIFFERENT MATERIALS

The approach has been confirmed on different materials, including on VITROPERM 500F from VAC (measured on W452 core). The model parameters are given in Table III. Measurements show promise that the approach is applicable for all material types, however, this remains to be confirmed as part of a future work.
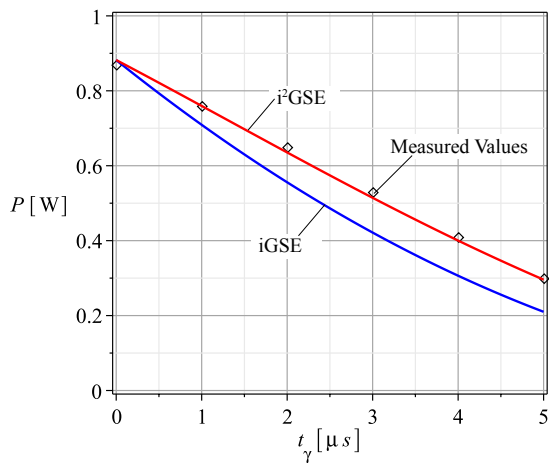
Fig. 10. Loss calculation and loss measurement comparison of the DAB example.

TABLE III
MODEL PARAMETER OF MATERIAL VITROPERM 500F (VAC).

α	1.88
β	2.02
k_i	$137 \cdot 10^{-6}$
α_r	0.76
β_r	1.70
k_r	$139 \cdot 10^{-6}$
τ	$9\,\mu s$
q_r	4

IX. CONCLUSION AND FUTURE WORK

The Steinmetz Equation (1) and its extension iGSE (2) are relatively accurate models to describe core losses. However, some core loss mechanisms cannot be described with an equation of only three parameters. The Steinmetz parameters alone are insufficient to fully describe core losses. This publication together with the work presented in [12] tries to show new approaches of how core losses could be better determined. However, a few new model parameters are necessary.

As experimentally verified, core losses are not necessarily zero when zero voltage is applied across a transformer or inductor winding after an interval of changing flux density. A short period after switching the winding voltage to zero, still losses occur in the material. This is due to magnetic relaxation. A new loss modeling approach has been introduced and named the *improved-improved Generalized Steinmetz Equation*, i²GSE. The i²GSE needs five new parameters to calculate new core loss components. Hence, in total eight parameters are necessary to accurately determine core losses.

The approach should be verified for different materials, applications, etc. Furthermore, a DC level of the antecedent flux density has not been part of this investigation of the present work and could be considered as part of a future work.

REFERENCES

[1] E. C. Snelling, *Soft Ferrites, Properties and Applications*. 2nd edition, Butterworths, 1988.
[2] J. Reinert, A. Brockmeyer, and R. De Doncker, "Calculation of losses in ferro- and ferrimagnetic materials based on the modified Steinmetz equation," *IEEE Transactions on Industry Applications*, vol. 37, no. 4, pp. 1055–1061, 2001.
[3] J. Li, T. Abdallah, and C. R. Sullivan, "Improved calculation of core loss with nonsinusoidal waveforms," in *Industry Applications Conference, 2001. 36th IEEE IAS Annual Meeting.*, vol. 4, pp. 2203–2210, 2001.
[4] K. Venkatachalam, C. R. Sullivan, T. Abdallah, and H. Tacca, "Accurate prediction of ferrite core loss with nonsinusoidal waveforms using only Steinmetz parameters," in *Proc. of IEEE Workshop on Computers in Power Electronics*, pp. 36–41, 2002.
[5] S. Iyasu, T. Shimizu, and K. Ishii, "A novel iron loss calculation method on power converters based on dynamic minor loop," in *Proc. of European Conference on Power Electronics and Applications*, pp. 2016–2022, 2005.
[6] T. Shimizu and K. Ishii, "An iron loss calculating method for AC filter inductors used on PWM inverters," in *Proc. of 37th IEEE Power Electronics Specialists Conference (PESC)*, pp. 1–7, 2006.
[7] K. Terashima, K. Wada, T. Shimizu, T. Nakazawa, K. Ishii, and Y. Hayashi, "Evaluation of the iron loss of an inductor based on dynamic minor characteristics," in *Proc. of European Conference on Power Electronics and Applications*, pp. 1–8, 2007.
[8] J. B. Goodenough, "Summary of losses in magnetic materials," *IEEE Transaction on Magnetics*, vol. 38, pp. 3398–3408, Sept. 2002.
[9] J. Liu, T. G. W. Jr., R. C. Wong, R. Wunderlich, and F. Lee, "A method for inductor core loss estimation in power factor correction applications," in *Proc. of Applied Power Electronics Conference and Exposition (APEC)*, 2002.
[10] C. R. Sullivan, J. H. Harris, and E. Herbert, "Core loss predictions for general PWM waveforms from a simplified set of measured data," in *Proc. of Applied Power Electronics Conference and Exposition (APEC)*, pp. 1048–1055, 2010.
[11] B. Carsten, "Why the magnetics designer should measure core loss; with a survey of loss measurement techniques and a low cost, high accuracy alternative," in *Proc. of PCIM*, pp. 163–179, 1995.
[12] J. Mühlethaler, J. Biela, J. W. Kolar, and A. Ecklebe, "Core losses under DC bias condition based on Steinmetz parameters," in *Proc. of the IEEE/IEEJ International Power Electronics Conference (ECCE Asia)*, pp. 2430–2437, 2010.
[13] *Ferrites and Accessories, Edition 2007.* EPCOS AG.
[14] G. Bertotti, *Hysteresis in Magnetism*. Academic Press, Inc., 1998.
[15] S. Chikazumi, *Physics of Ferromagnetism*. Oxford University Press, 1997.
[16] I. Villar, U. Viscarret, I. Etxeberria-Otadui, and A. Rufer, "Global loss evaluation methods for nonsinusoidally fed medium-frequency power transformers," *IEEE Transactions on Industrial Electronics*, vol. 56, pp. 4132–4140, Oct. 2009.
[17] F. Krismer and J. W. Kolar, "Accurate power loss model derivation of a high-current dual active bridge converter for an automotive application," *IEEE Transactions on Industrial Electronics*, vol. 57, no. 3, pp. 881 – 891, 2010.